Perfect Solid and Liquid

Bulletin of Research Center for Computing and Multimedia Studies,
Hosei University, **27** (2013)
Published online (http://hdl.handle.net/10114/8197)

Perfect Solid and Liquid

Yosuke Kataoka and Yuri Yamada
Department of Chemical Science and Technology, Faculty of Bioscience and Applied Chemistry,
Hosei University, 3-7-2 Kajino-cho, Koganei, Tokyo 184-8584, Japan
E-mail: yosuke.kataoka.7t@stu.hosei.ac.jp

SUMMARY

A 3-phase equilibrium in argon is obtained by the thermodynamics of the perfect solid and liquid. The equation of state (EOS) for a perfect solid is obtained for a pure substance of spherical molecules that undergo molecular interaction of the Lennard-Jones form. The primitive internal energy EOS for a perfect solid (referred to as v0 EOS) is the sum of the thermally averaged kinetic energy and the potential energy of the nearest neighbors in a face-centered cubic (FCC) solid at 0 K. The extended internal energy EOS for a perfect solid (v1) includes a long-range effect in the low density region as the internal energy in the van der Waals EOS. The pressure EOS is written as the volume derivative of the potential energy at 0 K to satisfy the EOS with respect to thermodynamics. The temperature effect in the virial term is included in the extended pressure EOS. The EOS for a perfect liquid is the van der Waals EOS with empirical coefficients to explain the 3-phase equilibrium. The change in entropy for a reversible process is calculated by the standard method. The thermodynamic quantities of each phase are written as functions of volume and temperature. In this way, the Gibbs energy per molecule is plotted as a function of pressure for both solid and liquid phases, and the crossing point in the plot is the phase transition point. The *p*-*V*-*T* relations on the equilibrium lines are comparable with the experimental and molecular simulation results. The calculated average potential energy and entropy on the phase boundaries are consistent with the simulations. The thermodynamic quantities under a low pressure are compared with the molecular dynamic simulations. The quantities examined are volume, internal energy, enthalpy, entropy, Helmholtz energy, Gibbs energy, expansion coefficient, isothermal compressibility and heat capacity under a constant pressure.

KEY WORDS: equation of state, phase diagram, triple point, critical constants, gibbs energy

1. INTRODUCTION

The perfect (ideal) solid and liquid are simplified models of a solid and a liquid composed of single-type spherical molecules. These models are used to understand 3-phase equilibrium through simplified calculations of Gibbs energies. Molecular interactions of the Lennard-Jones (LJ) form [1] are assumed for the spherical molecules. The LJ potential, $u(r)$, is expressed as a function of the interatomic distance, r:

$$u(r) = 4\varepsilon\left[\left(\frac{\sigma}{r}\right)^{12} - \left(\frac{\sigma}{r}\right)^{6}\right], \tag{1}$$

where ε is the depth of the potential well and σ is the separation at which $u(\sigma) = 0$. The ε and σ constants are used as units of energy and length, respectively.

The EOS for a perfect solid obtained in our previous study [2] and the van der Waals EOS were applied to the 3-phase equilibrium of argon [3]. The present work employs empirical van der Waals coefficients. The average potential energy function of the solid phase is improved by appropriate summation of the LJ potential.

Reasonable results obtained for the phase transition pressure as a function of temperature will be compared with the experimental results [4-7] and molecular dynamics (MD) simulations [8-15]. The thermodynamic quantities under a low pressure will be compared with the MD simulations [16].

Received 9 March 2013
Published online 30 June 2013

2. **Perfect solid**

The extended EOS for a perfect solid is expressed for a state with volume V, and temperature T; the most important term in the internal energy is the potential energy of the FCC solid at 0 K:

$$\frac{E_p(V,0\,\mathrm{K})}{\varepsilon N} = f_e\left[6.05\left(\frac{\sigma^3}{v}\right)^4 - 14.4\left(\frac{\sigma^3}{v}\right)^2\right], \qquad v \equiv \frac{V}{N}, \tag{2}$$

where N is the number of molecules in the system and v is the volume per molecule. This form is obtained by summation of the LJ system. The structure of a perfect solid can be expanded or compressed uniformly.

The potential energy at 0 K is modified to express the low density limit with a better approximation in v1 EOS [3]. The following weight functions are assumed in the low and high density regions:

$$w_\infty(v) = 1 - \frac{\sigma^3}{v}, \qquad w_\mathrm{s}(v) = \frac{\sigma^3}{v}. \tag{3}$$

The following long- and short-range force effects on the potential energy are assumed:

$$E_\infty(v) = -\frac{Na}{v}, \qquad E_\mathrm{s}(v) = E_\mathrm{p}(V,0\,\mathrm{K}). \tag{4}$$

The long-range effect is the internal energy in the van der Waals EOS [17, 18]. The potential energy in the present EOS is expressed as:

$$U_{e,s}(V,0\,\mathrm{K}) = w_\infty(v)E_\infty(v) + w_\mathrm{s}(v)f_eE_\mathrm{s}(v). \tag{5}$$

where the f_e factor (≈ 1) is introduced as an adjustable parameter.

The internal energy of the extended EOS for a perfect solid is the sum of the thermally averaged kinetic energy and the potential energy:

$$U(V,T) = \frac{3}{2}NkT + U_{e,s}(V,0\,\mathrm{K}), \tag{6}$$

where k is the Boltzmann constant.

The extended pressure EOS for a perfect solid is given as [2]:

$$p(V,T) = \frac{NkT}{V} - \left(\frac{\partial E_{\mathrm{p,ext}}(V,0\,\mathrm{K})}{\partial V}\right)_T + \frac{6\sigma^3 NkT}{V^2}. \tag{7}$$

The last term is obtained from a harmonic approximation of the following virial expression for the pressure [16]:

$$pV = NkT + \langle Virial\rangle_{T=0\,\mathrm{K}} + w_s(v)\langle Virial\rangle_{T>0}. \tag{8}$$

This form of Eq. (7) satisfies the thermodynamic EOS [1]:

$$\left(\frac{\partial U}{\partial V}\right)_T = T\left(\frac{\partial p}{\partial T}\right)_V - p. \tag{9}$$

The entropy change by a reversible process can be obtained by standard thermodynamics [1] using these EOSs:

$$\Delta S = Nk\ln\frac{V}{N\sigma^3} + \frac{3}{2}Nk\ln\frac{T}{\varepsilon/k} - \frac{6\sigma^3N^2k}{V} - S_0. \tag{10}$$

The starting point is selected as $V_i = Nv_{max}$, $T_i = \varepsilon/k$, where $v_{max} >> \sigma^3$. The S_0 constant is defined as:

$$S_0 \equiv S(Nv_{max}, \varepsilon/k) \equiv Nk \ln \frac{v_{max}}{\sigma^3}. \tag{11}$$

3. **Perfect liquid**

The van der Waals EOS [1] for a perfect liquid (v1) has the following form:

$$p(V,T) = \frac{kT}{v-b} - \frac{a}{v^2}, \quad v \equiv \frac{V}{N}, \tag{12}$$

where a and b are the van der Waals coefficients [1]. The internal energy of the van der Waals EOS is expressed as follows [17, 18]:

$$U(V,T) = \frac{3}{2}NkT - \frac{aN}{v}. \quad v \equiv \frac{V}{N}. \tag{13}$$

The change in entropy for the reversible process is calculated according to [1]:

$$\begin{aligned} \Delta S &= S(V,T) - S(Nv_{max}, \varepsilon/k) \\ &= Nk \ln \frac{v-b}{\sigma^3} + \frac{3}{2}Nk \ln \frac{T}{\varepsilon/k} - S_0. \end{aligned} \tag{14}$$

Here, the S_0 constant is the same as that in Eq. (10) and is selected as the origin of entropy in the present numerical calculation:

$$S_{fluid}(V,T) = Nk \ln \frac{v-b}{\sigma^3} + \frac{3}{2}Nk \ln \frac{T}{\varepsilon/k}, \tag{15}$$

$$S_{solid}(V,T) = Nk \ln \frac{v}{\sigma^3} + \frac{3}{2}Nk \ln \frac{T}{\varepsilon/k} - \frac{6\sigma^3 Nk}{v}. \tag{16}$$

The entropy of a perfect gas is also expressed for the case of $b = 0$ in Eq. (15):

$$S_{gas}(V,T) = Nk \ln \frac{v}{\sigma^3} + \frac{3}{2}Nk \ln \frac{T}{\varepsilon/k}. \tag{17}$$

The origin of potential energy is selected as zero when there is no interaction in either the solid or liquid phase.

The Gibbs energy G is obtained by the standard thermodynamic procedure:

$$G = U + pV - TS. \tag{18}$$

The liquid-gas critical points are known [1] as follows:

$$\begin{aligned} T_c &= \frac{8a}{27kb}, \\ p_c &= \frac{a}{27b^2}, \\ v_c &= 3b. \end{aligned} \tag{19}$$

The LJ parameters for argon [1] are given in Table 1. The empirical van der Waals coefficients are shown in units of LJ parameters in Table 2. Table 3 compares the critical points with the experimental results for argon [1]; the empirical van der Waals coefficients are determined according to the critical temperature and critical pressure.

Table 1. LJ parameters [1]

(ε/k)/K	$\varepsilon/10^{-21}$ J	$\sigma/10^{-10}$ m	(ε/σ^3)/MPa	(ε/σ^3)/atm
111.84	1.54	3.623	32.5	320

Table 2. Empirical van der Waals coefficients in units of LJ parameters [1]

$a/\varepsilon\sigma^3$	b/σ^3
5.087	1.117

Table 3. Comparison of the critical constants of argon obtained from EOS, MD simulation, and experiment [1]

	T_c/K	p_c/atm	V_c/(cm^3/mol)
EOS v1 [3]	133	47	86
This work	151	48	96
MD [15]	148	41	91
Exp. [1]	151	48	75

4. **Phase equilibrium in the (*T*-*p*) space**

The condition of the phase equilibrium between phases 1 and 2 in the (T-p) space is expressed as:

$$\begin{aligned} p_1(V_1, T) &= p_2(V_2, T), \\ \frac{G_1(V_1, T)}{N_1} &= \frac{G_2(V_2, T)}{N_2}. \end{aligned} \tag{20}$$

The EOSs are known as functions of volume and temperature; therefore, this equation can be solved numerically [2, 3]. An example of this is shown in Fig. 1 at $T = 0.692\ \varepsilon/k$. The branch with the lowest chemical potential G/N, at a given pressure is the phase that is realized at this temperature and pressure. The intersection point indicates the phase transition pressure at the given temperature. In the case of $T = 0.692\ \varepsilon/k$, the transition pressure for the solid-liquid transition is $p = 4.97\times10^{-3}\ \varepsilon/\sigma^3$. This is also the liquid-gas and solid-gas transition

point, as shown in Fig. 1. The gas phase is most stable in the lowest pressure region; therefore, the solid phase will be realized if the pressure is increased sufficiently at this temperature. The temperature $T = 0.692\ \varepsilon/k$ is the triple point and this is compared with the experimental results in Table. 4. The pressure p_3, is higher and the change in enthalpy for the solid-liquid transition is larger than the experimental value. Some comments will be given on the enthalpy of the liquid phase in the next section. The mass density of the liquid is reasonable. The adjustable parameter in Eq. (2) is fixed in an attempt to reproduce the triple point obtained by Monte Carlo (MC) simulation [12].

$$f_e = 0.9088522 \tag{21}$$

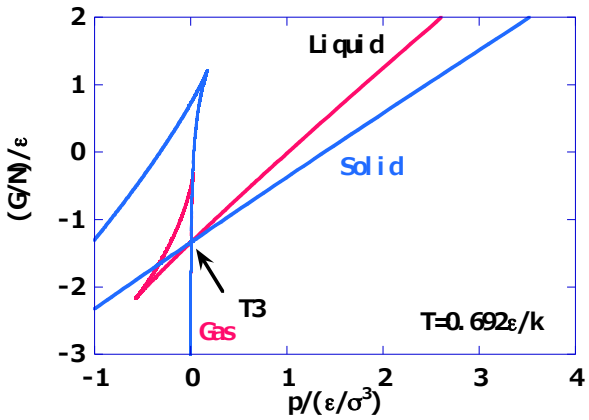

Fig.1 Gibbs energy per molecule G/N, vs. pressure at $T_3 = 0.692\ \varepsilon/k$. The triple point is indicated by an arrow.

Table 4. Comparison of the EOS, MC simulation and experimental triple points [4]. The mass density of the liquid ρ_L, and the change in enthalpy for the solid-liquid transition $\Delta_{SL}H$, are also given

	T_3/K	p_3/atm	ρ_L/(g/cm^3)	ΔH_{SL}/(J/g)
EOS v1 [3]	69.2	1.75	1.13	60.5
This work	77.4	1.59	1.02	94
MC [12]	77.4	0.32	1.18	26
Exp. [4]	83.8	0.68	1.42	28

The transition pressure is plotted as a function of temperature in Fig. 2 and compared with the experimental [5-7] and simulation [8-15] results for argon. The pressure-axis is presented as a logarithmic scale, because the range is very wide. The overall transition pressure for argon is well reproduced as a function of temperature.

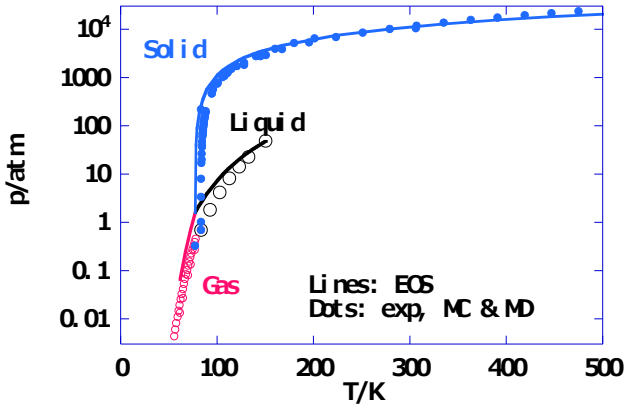

Fig. 2 Phase transition pressure vs. temperature for argon. Comparison of the EOS, experimental [5-7], and

simulation [8-15] results.

Fig. 3 shows the transition temperature-number density relation for argon, and the calculated results are compared with the simulation results [8-15]. The phase boundaries of the liquid and solid branches obtained from EOS calculations deviate from the simulation results at high temperatures. The most important reason for this is the hard sphere term in the pressure equation for the liquid. The differences in the transition temperature-number density plot may be improved by the other EOS for the LJ system.

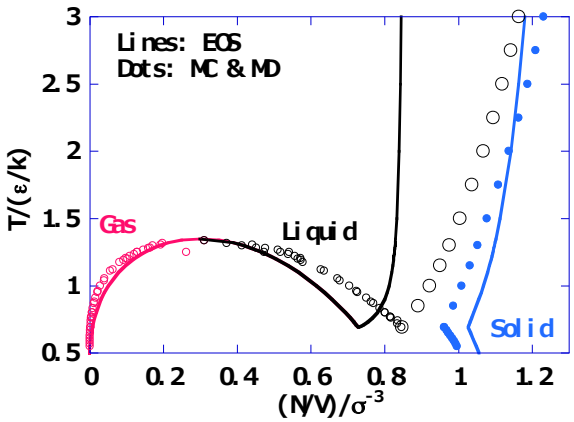

Fig. 3 Phase transition temperature vs. number density for argon. Comparison of the EOS and simulation results [8-15].

The calculated configurational entropy per molecule S_c/N, is compared with the simulation results [12] in Fig. 4. The configurational entropy has the following form in the present model:

$$S_{\mathrm{c,solid}}(V,T) = Nk\ln\left(\frac{V}{N\sigma^3}\right) - \frac{6\sigma^3N^2k}{V} + Nk \tag{22}$$

$$S_{\mathrm{c,fluid}}(V,T) = Nk\ln\frac{v-b}{\sigma^3} + Nk. \tag{23}$$

The overall features of the configurational entropy from the EOS are in good agreement with the simulation results [12]. Some differences in the liquid and solid phases at high temperatures are due mainly to differences in the volume.

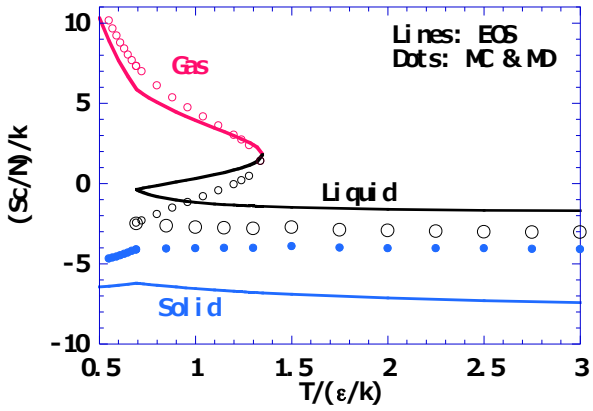

Fig. 4. Configurational entropy per molecule S_c/N, vs. temperature for the phase equilibrium of argon. Comparison of the EOS and simulation results [12].

The average potential energies per molecule U_e/N, at the phase boundaries are shown in Fig. 5:

$$U_{\mathrm{e,solid}} = E_{\mathrm{p,s}}(V, 0\mathrm{K}) \tag{24}$$

$$U_{\mathrm{e,fluid}} = -\frac{aN^2}{V}. \tag{25}$$

The potential energies of the solid and gas at low temperatures correspond well with the simulation results [12]. However, the potential energies of the liquid and the solid at high temperatures are different from the observed results [12], because the present EOS potential energy terms have no explicit temperature dependence (see Eqs. (24) and (25)). Improvement of this weakness is a target for future study. The average potential energy of the harmonic oscillator is *kT/2* at temperature *T*, for each degree of freedom of motion. This term is not included in the present study. A volume dependent term is expected in the next version of EOS, such as *g(V)kT*, where *g(V)* is a function of volume.

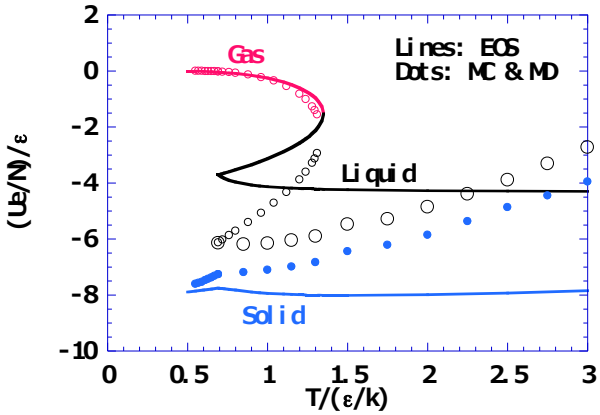

Fig. 5. Average potential energy per molecule U_e/N, vs. temperature for the phase equilibrium of argon. Comparison of the EOS and simulation results [12].

Fig. 6 describes the configurational Helmholtz energy A_c, as a function of temperature on the solid-liquid phase boundaries. The tangent of the calculated A_c corresponds to that of the MC simulation result [12]. However, some improvements are necessary for A_c in the liquid phase.

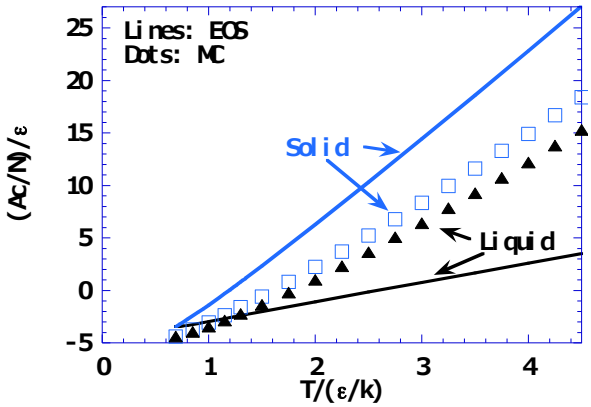

Fig. 6. Configurational Helmholtz energy per molecule A_c/N, vs. temperature for the solid-liquid equilibrium of argon. Comparison of the EOS and simulation results [12]. Squares and triangles represent the solid and liquid phases obtained by MC simulation [12], respectively.

Finally, A_c in the solid-gas phase boundary is compared with that from the MC simulation [12] in Fig. 7. The present EOS gives A_c values on the solid-gas phase boundary that are comparable with those obtained by MC simulation.

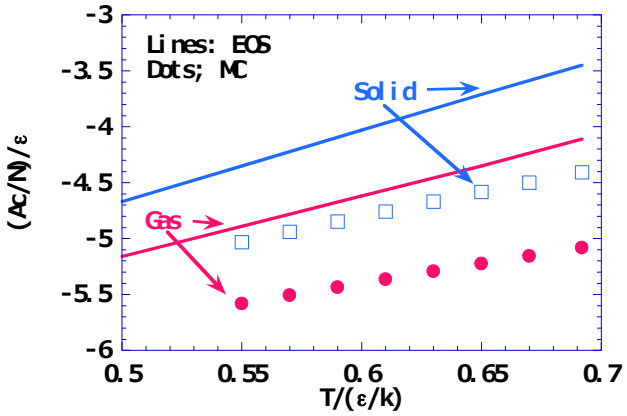

Fig. 7. Configurational Helmholtz energy per molecule A_c/N vs. temperature for the solid-gas equilibrium of argon. Comparison of the EOS and simulation results [12].

5. **Thermodynamic properties at constant pressure**

The thermodynamic quantities under low pressures are examined in this section for comparison of the EOS and simulation results. The Gibbs energy is plotted in Fig. 8 as a function of temperature at $p = 0.01\ \varepsilon/\sigma^3$. The entropies of the liquid and solid are negative, due to the present choice of the origin of entropy; therefore, this plot appears different from the typical *G*-*T* plot [1]. The melting point T_m, and the boiling point T_b, are fixed in Fig. 8:

$$T_m = 0.692\ \varepsilon/k,\ T_b = 0.77\ \varepsilon/k \tag{26}$$

The EOS results are compared with the Kolafa-Nezbeda (KN) EOS determined from many simulation results on the LJ system [13]. Some differences are evident in the liquid branch, which indicates the differences between the van der Waals EOS and the LJ system.

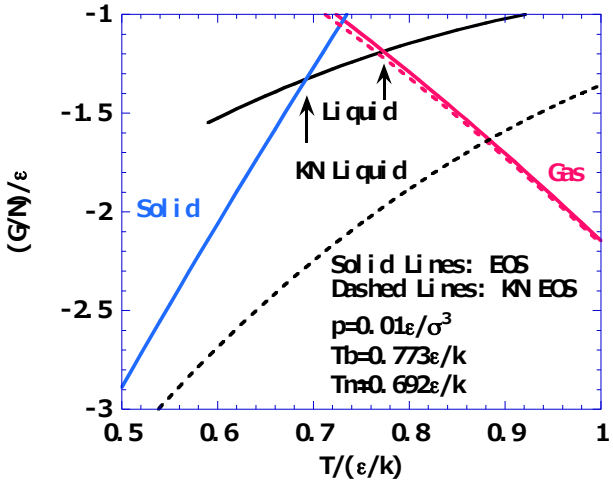

Fig. 8. Gibbs energy per molecule vs. temperature at $p = 0.01\ \varepsilon/\sigma^3$. Comparison of the EOS and KN EOS simulation results [13]. The melting point is 0.692 ε/k and the boiling point is 0.77 ε/k.

Fig. 9 shows the volume per molecule as a function of temperature at $p = 0.01\ \varepsilon/\sigma^3$. The solid branch is compared with the present MD results. The MD simulation is performed on an 864 particle system using a standard NTP ensemble [16].

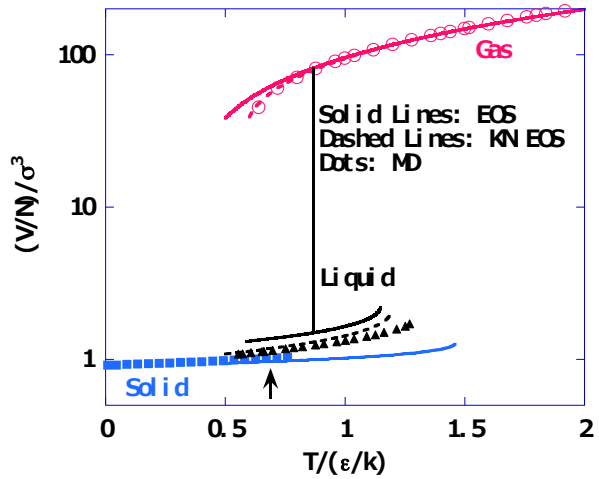

Fig. 9. Volume per molecule vs. temperature at $p = 0.01\ \varepsilon/\sigma^3$. Comparison of the EOS and KN EOS simulation results [13], including the MD simulation results from this study.

The internal energy is plotted in Fig. 10. The internal energy of the liquid is slightly different from the simulation results for the LJ system, because the EOS calculation is based on the van der Waals EOS. Therefore, another EOS will be developed for the liquid phase in a future study. The difference in the internal energy of the solid phase originates from the approximation that the potential energy has no temperature dependence, which is invoked for simplicity. This should be improved by the following research.

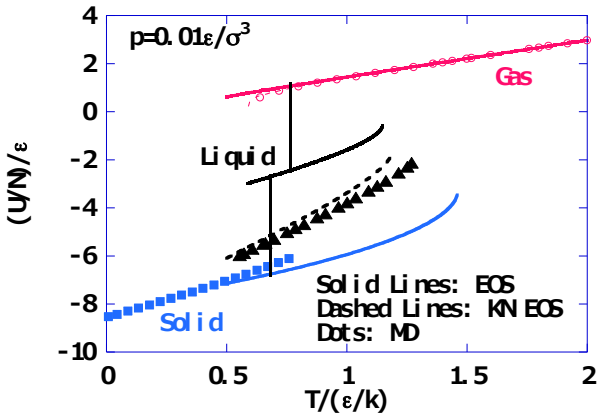

Fig. 10. Internal energy per molecule vs. temperature at $p = 0.01\ \varepsilon/\sigma^3$. Comparison of the EOS and simulation results [13], including the MD simulation results from this study.

Fig. 11 shows the enthalpy per molecule vs. temperature at $p = 0.01\ \varepsilon/\sigma^3$. The EOS calculation is based on the van der Waals EOS, and thus the calculated enthalpy of the liquid is different from the simulation results for the LJ system.

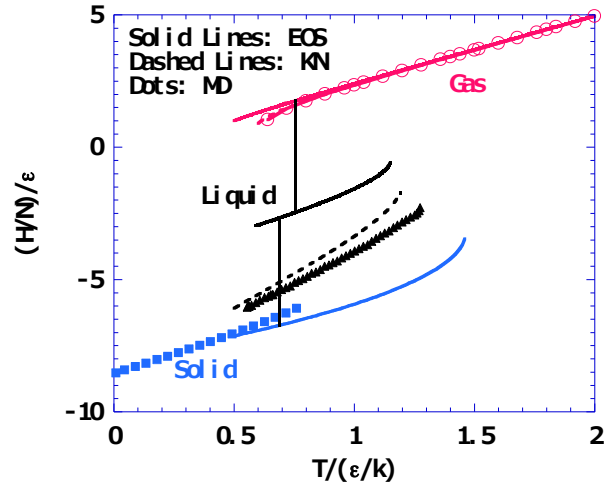

Fig. 11. Enthalpy per molecule vs. temperature at $p = 0.01\ \varepsilon/\sigma^3$. Comparison of the EOS and simulation results [13], including the MD simulation results from this study.

The Helmholtz energy per molecule is shown in Fig. 12 for completeness and the entropy per molecule is presented in Fig. 13. The entropy of the liquid obtained by EOS is close to that for the simulations. The entropies of the liquid and solid are both negative due to the present choice of the origin of entropy.

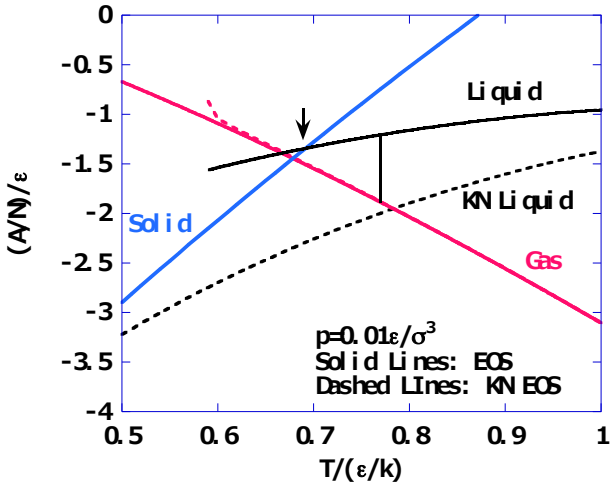

Fig. 12. Helmholtz energy per molecule vs. temperature at $p = 0.01\ \varepsilon/\sigma^3$. Comparison of the EOS and KN EOS simulation results [13].

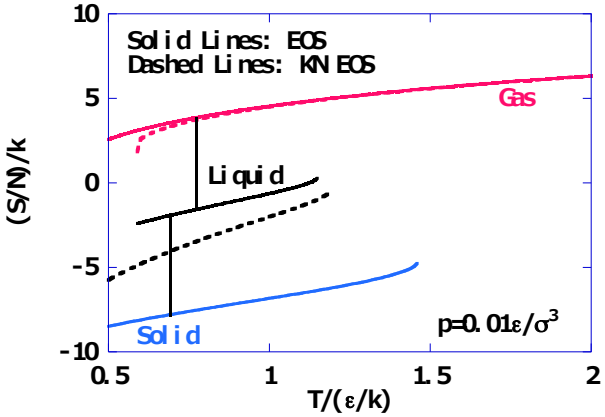

Fig. 13. Entropy per molecule vs. temperature at $p = 0.01\ \varepsilon/\sigma^3$. Comparison of the EOS and KN EOS simulation results [13].

Fig. 14 compares the expansion coefficient α, calculated by EOS with that obtained from the simulations. Although α for the liquid and solid are slightly different from those obtained by the simulations, the overall features are similar.

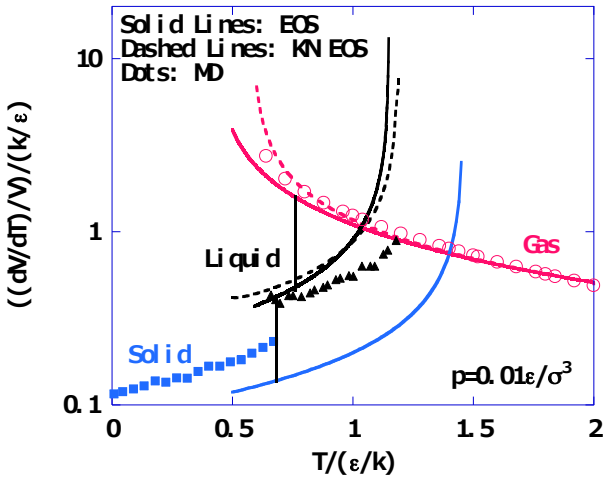

Fig. 14. Thermal expansion coefficient vs. temperature at $p = 0.01\ \varepsilon/\sigma^3$. Comparison of the EOS and simulation results [13], including the MD simulation results from this study.

The isothermal compressibility κ_T, obtained by EOS is plotted in Fig. 15. κ_T of the solid calculated by EOS is slightly larger than that obtained by MD simulation. Thus, some improvement in the EOS of the solid is necessary to achieve better coincidence of κ_T.

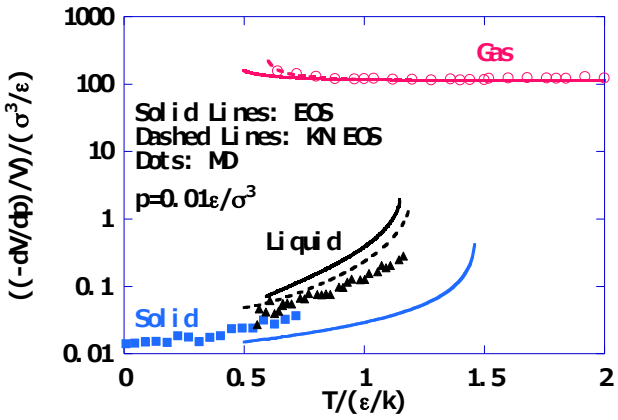

Fig.15. Isothermal compressibility κ_T, vs. temperature at $p = 0.01\ \varepsilon/\sigma^3$. Comparison of the EOS and simulation results [13], including the MD simulation results from this study.

Fig. 16 shows the heat capacity under a constant pressure, *Cp*. The main reason for the difference between the calculated heat capacities of the solid and the liquid and those obtained by MD simulation is that the EOS neglects the explicit temperature dependence in the potential energy of the condensed phase.

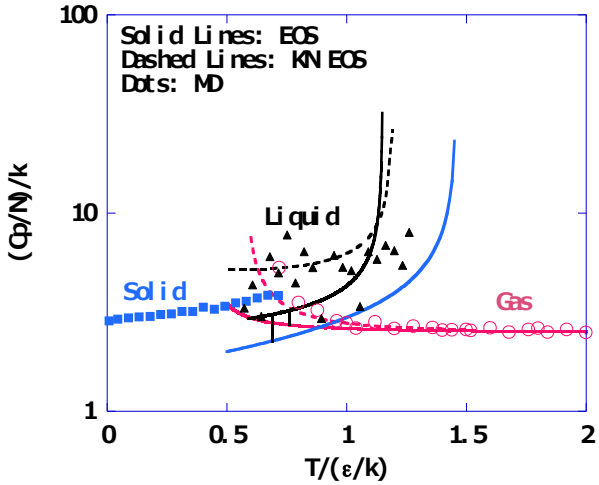

Fig. 16. Heat capacity at constant pressure per molecule (C_p/N) vs. temperature at $p = 0.01\ \varepsilon/\sigma^3$. Comparison of the EOS and simulation results [13], including the MD simulation results from this study.

6. CONCLUSIONS

The phase transitions in the three phases of argon are well reproduced by EOSs for a perfect solid and the empirical van der Waals fluid. The potential energy for argon can be expressed by the LJ pair potential. For this reason, the LJ potential parameters, ε and σ, are not adjustable parameters. Only the f_e factor in the potential energy of the solid and the van der Waals parameters a and b are adjustable parameters in the present EOS. It is expected that optimization of these parameters will provide improved results that are comparable with the experimentally observed results. The EOS for a perfect solid has a simple analytic form. The van der Waals EOS is also easily understood. A set of these EOSs is expected to be employed for thermodynamic education in physical chemistry. Some worksheets for the Gibbs energy calculation are available on request to the author (YK).

ACKNOWLEDGMENT

The authors would like to thank the Research Center for Computing and Multimedia Studies of Hosei University for the use of computer resources.

APPENDIX

Some examples of worksheets for the Gibbs energy calculation are attached [18, 19] .

REFFERENCES

[1] P. W. Atkins, *Physical Chemistry*, Oxford Univ. Press, Oxford (1998).
[2] Y. Kataoka and Y. Yamada, *J. Comput. Chem. Jpn.*, **10**, 98-104 (2011).
[3] Y. Kataoka and Y. Yamada, *J. Comput. Chem. Jpn.*, **11**, 81-88 (2012).
[4] CRC Handbook of Chemistry and Physics, Ed. D. R. Lide, CRC press, Boca Raton (1995).
[5] The Chemical Society of Japan, *Kagaku-binran Kisohen*, *Kaitei-yonhan*, Maruzen, Tokyo (1993).
[6] R. K. Crawford and W. B. Daniels, *Phys. Rev. Lett.*, **21**, 367-369 (1968).
[7] W. van Witzenburg and J. C. Stryland, *Can. J. Phys.*, **46**, 811-816 (1968).
[8] J-P Hansen and L. Verlet, *Phys. Rev.*, **184**, 151-161 (1969).
[9] D. A. Kofke, *J. Chem. Phys.*, **98**, 4149-4162 (1993).
[10] R. Agrawal and D. A. Kofke, *Mol. Phys.*, **85**, 43-59 (1995).
[11] M. A. van der Hoef, *J. Chem. Phys.*, **117**, 5092-5093 (2002).
[12] M. A. Barroso and A. L. Ferreira, *J. Chem. Phys.*, **116**, 7145-7150 (2002).
[13] J. Kolafa and I. Nezbeda, *Fluid Phase Equilibr.*, **100**, 1-34 (1994).

[14] H. Okumura and F. Yonezawa, *J. Chem. Phys.*, **113**, 9162-9168 (2000).
[15] H. Okumura and F. Yonezawa, *J. Phys. Soc. Jpn.*, **70**, 1990-1994 (2001).
[16] M. P. Allen and D. J. Tildesley, *Computer Simulation of Liquids*, Clarendon Press, Oxford (1992).
[17] Y. Kataoka and Y. Yamada, *J. Comput. Chem. Jpn.*, **8**, 97-104 (2009).
[18] D. A. McQuarrie, *Statistical Mechanics*, Harper Collins (1976).
[19] T=1.000.xlsx, http://www.media.hosei.ac.jp/bulletin/vol27_03/T=1.000.xlsx
[20] RCCMS-p=0.01.xlsm, http://www.media.hosei.ac.jp/bulletin/vol27_03/RCCMS-p=0.01.xlsm

